Effect of Target Composition on Proton Energy Spectra in Ultraintense Laser-Solid Interactions

A. P. L Robinson,[1,2] A. R. Bell,[1] and R. J. Kingham[1]

[1]*Blackett Laboratory, Prince Consort Road, Imperial College London, London SW7 2BZ, United Kingdom*
[2]*Central Laser Facility, Rutherford-Appleton Laboratory, Chilton, Oxfordshire, OX11 0QX, United Kingdom*

(Received 10 November 2005; revised manuscript received 8 December 2005; published 27 January 2006)

We study how the proton density in a target irradiated by an ultraintense laser affects the proton spectrum, with analytical models and Vlasov simulations. A low relative proton density gives rise to peaks in the energy spectrum. Furthermore, a target with the protons confined to a thin, low density layer produces a quasimonoenergetic spectrum. This is a simple technique for producing proton beams with a narrow energy spread for proton radiography of laser-plasma interactions.

DOI: 10.1103/PhysRevLett.96.035005 PACS numbers: 52.38.Kd, 52.50.Jm, 52.59.−f, 52.65.Ff

The emission of multi-MeV protons from the rear surface of solid targets irradiated by ultraintense ($>10^{18}$ W cm^{-2}) lasers has been the subject of intense experimental [1–6], and theoretical investigation [7–12]. These protons beams are of great interest, because of their potential application to fast ignition [12], medicine [13], and particle accelerators [14]. Although other acceleration mechanisms have been suggested [1], the acceleration of the protons at the rear of the target by strong electrostatic fields is often regarded as the primary mechanism. Although a strong basic understanding of this exists [15,16], this currently does not give much insight into how the proton energy spectrum might be controlled. Three-dimensional (3D) particle-in-cell (PIC) simulations by Esirkepov [17] have demonstrated the production of quasimonoenergetic proton beams. Very recently, experiments done by Hegelich *et al.* demonstrated the production of quasimonoenergetic carbon ions using a very thin carbon coating [18]. This work is very encouraging, yet the underlying physics is not entirely clear. It is therefore necessary to extend the current theoretical understanding, and to confirm any new insights using suitable simulation codes, so that the proton energy spectrum can be manipulated. Control of the energy spectrum is necessary for the aforementioned applications.

In this Letter it is shown that by changing the composition of a homogeneous target composed of protons and one heavy ion species, the maximum proton energy is changed, and that a peak is produced in the proton spectrum. In the previous work of Esirkepov [17], the spectrum was attributed to both the low proton density and the thinness of the proton layer. The effect of varying the proton density was not explored, nor were the consequences for the achievable proton energies. In this Letter it is shown, for the first time, that the low proton density is the most important factor. The theoretical basis of the acceleration mechanism is explained, including a new model devised for the low proton density limit. The results of novel three-species relativistic Vlasov simulations, which are in excellent agreement with theory, are presented. The analytical theory explains the behavior only in the limits of very high and very low proton density. The Vlasov simulations are necessary to investigate intermediate densities. The theory implies that the maximum proton energy decreases as the proton density in the target is reduced, and this is confirmed by the Vlasov simulations. However, a definite peak emerges in the proton spectrum that increases in energy as the proton density is decreased, as predicted. New Vlasov simulations of inhomogeneous targets, where the protons are only confined to a thin layer at the target surface, are also reported. The results suggest that it is possible to produce quasimonoenergetic proton beams from a target where the protons are confined to a thin layer at the surface in which the proton density is low. This represents a promising route to manipulating the proton energy spectrum.

In order to analyze the effect of varying the proton density on the maximum proton energy and the energy spectrum, the two limits of the problem are considered. The simplest view of the electrostatic acceleration mechanism is to consider a plasma with hot electrons and cold ions which has a sharp interface with a vacuum. This is the problem that Gurevich considered in one dimension, and found a single, self-similar solution for (1). However, this was for a Maxwellian electron population that was described by a single temperature. In the case of a solid irradiated by an ultraintense laser pulse, the plasma is much better described as a two-temperature plasma. In this model the plasma has a cold electron population at density $n_{c,0}$ and temperature T_c, and a fast electron population which is generated by the laser interaction. This is at density $n_{f,0}$ and temperature T_f. In most experiments, $T_f \gg T_c$, and $n_{c,0} \gg n_{f,0}$. The fast electron temperature can be estimated from the ponderomotive potential energy of the laser pulse ($T_f \approx 511(\sqrt{1 + I\lambda^2/2.8 \times 10^{18}} - 1)$ where $I\lambda^2$ has units of W cm^{-2} μm^2) [19], and the fast electron density can be estimated from an energy balance.

In the high proton density limit, a single species, two-temperature expansion is required. In the low proton density limit, the same description is required (albeit the ion

species has a different charge-to-mass ratio), but it is now necessary to understand the motion of a "test proton" in the electric field established by the heavy ions.

The single species, one-temperature expansion is well understood [15,20]. The two-temperature expansion is less well understood, and it can be shown that a single self-similar solution is not possible if $T_f/T_c > 5 + \sqrt{24}$ [21]. It has, however, been suggested that a suitable analytic solution can be constructed from four separate solutions [16]. The four solutions are: (i) a cold rarefaction wave, (ii) a rarefaction shock, (iii) a region of ballistic flow, (iv) a fast rarefaction wave. The rarefaction wave solutions [(i) and (iv)] are those of the Gurevich solutions. The rarefaction shock [(ii)] is an electrostatic shock where the ion density changes discontinuously. The region of ballistic flow [(iii)] is a region of constant ion velocity.

Since the fast rarefaction wave is completely dominated by the fast electrons, and it is composed of the highest energy protons, the fast rarefaction wave is well described by a single temperature expansion. However the appropriate temperature must be the fast electron temperature, and the appropriate electron density must be the fast electron density in the undisturbed plasma. It is predicted here that for a pure-proton, two-temperature expansion, that the energy spectrum of the highest energy protons will be adequately described by the Gurevich formula, Eq. (1) [20], and that the maximum proton energy is adequately described by the Mora formula, Eq. (2) [15], with the fast electron temperature and density (T_f and $n_{f,0}$) being used in both formulas.

$$\frac{dN}{d\epsilon} = \frac{n_{f,0} c_s t}{Z\sqrt{2Zk_B T_f \epsilon}} \exp\left[-\sqrt{\frac{2\epsilon}{Zk_B T_f}} \right], \tag{1}$$

$$\epsilon_{\max} = 2Zk_B T_f [\ln(\tau + \sqrt{\tau^2 + 1})]^2. \tag{2}$$

In Eqs. (1) and (2), Z is the ion charge, ϵ is the proton energy, $c_s = \sqrt{Zk_B T/m_i}$ (m_i is the ion mass), $\omega_{\mathrm{pi}} = \sqrt{Zn_{f,0}e^2/m_i\varepsilon_0}$, and $\tau = \omega_{\mathrm{pi}} t/\sqrt{2e^1}$. Now the other limit is considered, where the protons are present only as a trace quantity, and the rest of the target is composed of heavy ions (i.e., $Ze/m_i < e/m_p$). In this situation the protons act as test particles, and the highest energy protons will always be ahead of the heavy ion front, as the heavy ions determine the electric field structure in this limit. In order to calculate the maximum proton energy as a function of time, we need to integrate the proton equation of motion in the sheath field at the heavy ion front. This requires knowing the electric field as a function of both x and t. Following the work of Passoni *et al.* [22], the electric field beyond the heavy ion front (i.e., for $x > x_i$, where x_i is the position of the heavy ion front) is determined by the nonlinear Poisson equation $\partial^2\phi/\partial x^2 = en_{f,0}\exp(e\phi/k_B T_f)/\varepsilon_0$. In this equation the cold electrons have been neglected, which is valid for most of the time during the expansion, and even at early times provided that $n_f T_f \gg n_c T_c$. This can be integrated to obtain Eq. (3), the boundary conditions being (i) $\partial\phi/\partial x \to 0$ as $x \to \infty$, (ii) $\phi(x_i) = \phi_0$. The electrostatic potential at the ion front is determined by matching the solution of the corresponding nonlinear Poisson equation for the interior of the target. In general it will be time dependent. However, for the sake of simplicity, the maximum proton energy for the optimum case ($\phi_0 = 0$) is calculated and compared to the pure-proton expansion.

$$E = \frac{\sqrt{2}k_B T_f}{e\lambda_{D,f}} e^{(e\phi_0/2k_B T_f)} \left[1 + \frac{(x - x_i)}{\sqrt{2}\lambda_{D,f}} e^{(e\phi_0/2k_B T_f)} \right]^{-1}. \tag{3}$$

For this calculation, the fast electron density is $n_f = 10^{27}\ \mathrm{m}^{-3}$, and the fast electron temperature is $T_f = 1.5$ MeV. For a heavy ion species C^{4+} is used. Note that x_i is given by the formula that Mora gives [15]. The maximum proton energy for a pure-proton expansion is calculated from Eq. (2), and the maximum proton energy for low density proton acceleration according to the "moving sheath" model that has just been described, is plotted in Fig. 1.

Figure 1 shows that the maximum proton energy in the pure-proton expansion quickly becomes larger than that of the low density sheath accelerated protons. However this cannot be taken as a definitive answer, as the difference in energy is only factor of 2, between the two models. Given the number of assumptions that were made, more sophisticated calculations are required to have greater confidence in this result. Between the two limits the maximum proton energy is expected to change monotonically (i.e., for the maximum proton energy to decrease with decreasing proton density), but actual kinetic simulations are required to

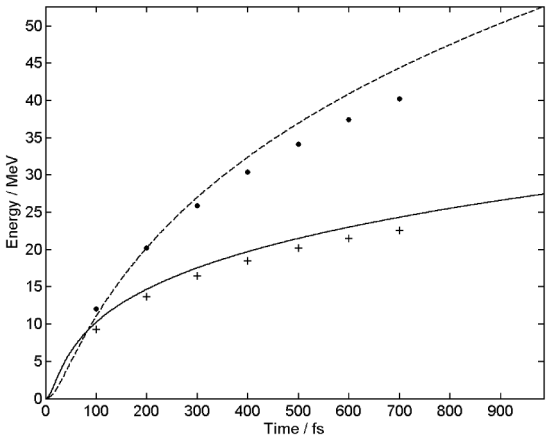

FIG. 1. Comparison of maximum proton energy of 100% (dot) and 0.1% (cross) composition simulations with the Mora expression (dashed line) and moving sheath model (solid line), respectively.

confirm this. The proton spectrum must also be different in the low density limit. If the protons are behaving as test particles then the effect of the sheath field at the heavy ion front must be to produce a peak in the proton spectrum, as the protons that lie close to the initial plasma-vacuum interface must all experience approximately the same time-integrated electric field. This effect on the spectrum also needs to be checked by kinetic simulation.

To answer these questions a set of simulations were carried out using a three-species, relativistic Vlasov solver. The code has one spatial and one momentum dimension (1D1P). The simulations contained no laser physics. Instead the target was treated as a planar plasma, with the fast electron density and temperature being uniform throughout. This is essentially the configuration normally considered analytically, however the ''reservoir'' of fast electrons is now finite in extent. This code solves $\partial f_\alpha/\partial t + (p_x/\gamma m_\alpha)\partial f_\alpha/\partial x + q_\alpha E \partial f_\alpha/\partial p = 0$, and is coupled to Ampère's Law ($\partial E/\partial t = -\sum_\alpha j_\alpha/\varepsilon_0; \nabla \times \mathbf{B} = 0$) for the electric field. α denotes one of the three particle species: electrons (e), protons (p), and heavy ions (i). The code uses nonuniform grids in both space and momentum to resolve the necessary scales, and simultaneously provide a sufficiently large grid. Reflective boundaries are used in space.

The code was initialized with a uniform plasma from 0 to 86 μm, and vacuum from 86 to 400 μm. This plasma was a relativistic bi-Maxwellian with $T_c = 10$ keV and $T_f = 1.5$ MeV. The electron densities were $n_c = 10^{29}$ m^{-3} and $n_f = 3.5 \times 10^{27}$ m^{-3}. Simulations were run with a proton composition, g, of 100%, 66%, 50%, 25%, 10%, 1%, and 0.1%. Note that this is composition by number density [i.e., $g = n_p/(n_p + n_C)$]. The simulations were run for 700 fs.

First the general features observed in the simulations are described. Figure 2 shows the electric field at 400 fs in the 66% simulation. In this figure a set of features have been labeled from A–E. Feature A is the cold rarefaction wave, which propagates into the target at the cold ion acoustic velocity. Feature B is the rarefaction shock described by Bezzerides [23] and Tikhonchuk [16]. The regions labeled C are the fast rarefaction waves, and are regions of self-similar expansion where the fast electrons dominate. Feature D is the electrostatic shock at the C^{4+} front, and E is the electrostatic shock at the proton front.

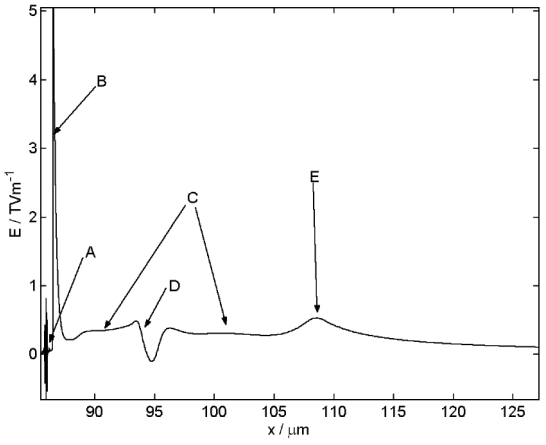

FIG. 2. Electric field at 400 fs in 66% composition simulation.

It has been found that the maximum proton energy is highest in the 100% simulation and decreases almost monotonically with proton density. A ''primary'' peak in the proton spectrum is observed, that is always present, and the energy at which this peak sits increases with decreasing proton density. At very low proton density, the primary peak lies at the maximum proton energy as predicted. This peak is due to protons being accelerated across the electrostatic shock at the C^{4+} front (feature D in Fig. 2). At high proton density, this electrostatic shock is weak due to proton screening. As the proton density decreases the shock becomes stronger and the energy of the primary peak correspondingly increases. At extremely low proton density, the C^{4+} front is essentially a plasma-vacuum interface, and this is the strongest electrostatic shock that can be produced. The rarefaction shock causes a very low ''secondary'' energy peak, however it is the shock at the C^{4+} front that causes the primary peak in the proton spectrum. In Fig. 3 the proton spectra at 700 fs for the 100%, 50%, 25%, and 1% simulations are shown.

In the case of the 100% composition simulation, the dependence of the maximum proton energy on time closely matched Eq. (2). In the case of the 0.1% simulation the maximum proton energy's time dependence is well described by the moving sheath model for $\phi_0 = 0$. Both of these results are shown in Fig. 1. This shows that the simulations have validated the analytical models that were described earlier for the maximum proton energy.

At all proton densities, the lower energy part of the spectrum is due to protons that originate further from the initial plasma-vacuum interface. If the protons are confined to a thin surface layer, then the lower energy part of the spectrum must be altered. In the case of a low proton density surface layer, this will eliminate the lower energy part of the spectrum to produce a quasimonoenergetic

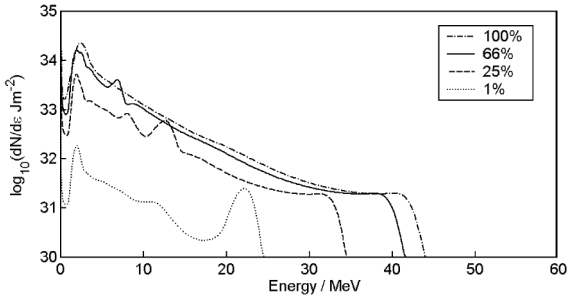

FIG. 3. Proton energy spectra at 700 fs for 100%, 66%, 25%, and 1% composition simulations.

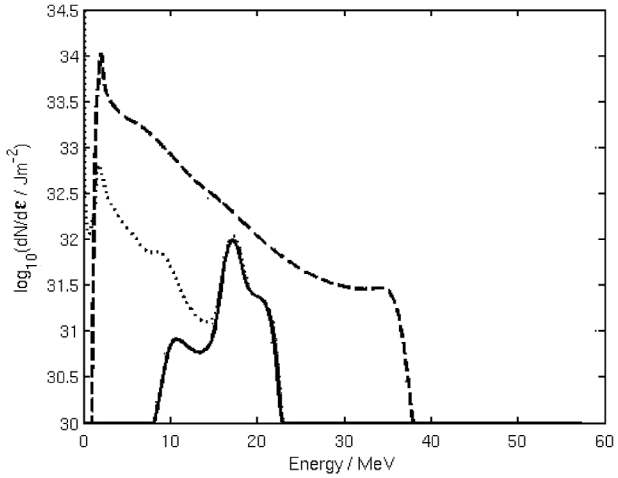

FIG. 4. Proton spectra of 100% (dashed line) and 5% (solid line) inhomogeneous targets at 500 fs. Spectrum of a target with a 100 nm, 5% proton layer is shown for comparison (dotted line).

spectrum. In the case of a high proton density surface layer, the spectrum remains broad due to the very low cold acoustic velocity, and the very small cold Debye length. To investigate this, two additional simulations were carried in which the protons were only present in a 10 nm surface layer. The rest of the target was 100% C^{4+}. In one simulation the proton layer was 5% protons, and 100% protons in the other. The spectra at 500 fs of both simulations are shown in Fig. 4. In the case of the 100% simulation the spectrum is still Gurevich-like. Despite making the surface layer very thin, it is still thicker than the cold Debye length ($\lambda_{D,c} \approx 1$ nm) and a plasma expansion still occurs. In the case of the 5% target we have obtained a quasimonoenergetic spectrum. This emphasizes why the low proton density, and not the layer thickness is crucial to obtaining the quasimonoenergetic spectrum. An additional simulation was carried out with a 100 nm, 5% proton layer, the resulting spectrum is also shown in Fig. 4. This shows that the protons that contribute to the peak come from the first 10 nm.

One should ask whether producing monoenergetic protons by this method is advantageous in terms of applications, i.e., whether it is possible to produce higher $dN/d\epsilon$ using this method. Figs. 3 and 4 show that the peak $dN/d\epsilon$ in low proton density targets is often less than or comparable to the $dN/d\epsilon$ at the same energy in the high density targets. However the factor between the two values is less than the ratio of the proton densities in the two targets. Nonetheless, this method of controlling the proton spectrum is not useful for all applications. However for applications where monoenergetic protons are required, and post-acceleration selection is *not* possible, then this could be a very useful method.

Other parameters were also varied—a lower charge-to-mass ratio (q/m) of the heavy ions resulted in both a lower proton energy (as expected from the analytical model) and a much broader spectrum. This was due to proton expansion far from the ion front. We also considered a more arbitrary proton density profile. These results will be reported on, in more detail, in a future publication.

In conclusion, we have demonstrated that, in a 1D two-temperature plasma expansion with two ion species, the reduction of the relative proton density produces a peak in the proton energy spectrum due to the increasing strength of the electrostatic shock at the heavy ion front. Furthermore, we have also shown that when the protons are confined to a thin surface layer, and the relative proton density is low, a quasimonoenergetic energy spectrum is produced. This shows that, by controlling the target composition, the proton energy spectrum can be controlled. Proton radiography [24] of laser-plasma interactions is one such application where this will be particularly useful.

This work was supported by the UK Engineering and Physical Sciences Research Council.

[1] E. L. Clark *et al.*, Phys. Rev. Lett. **84**, 670 (2000).
[2] R. A. Snavely *et al.*, Phys. Rev. Lett. **85**, 2945 (2000).
[3] A. Maksimchuk *et al.*, Phys. Rev. Lett. **84** 4108 (2000).
[4] A. J. Mackinnon *et al.*, Phys. Rev. Lett. **86** 1769 (2001).
[5] A. J. Mackinnon *et al.*, Phys. Rev. Lett. **88** 215006 (2002).
[6] M. C. Kaluza, Ph.D. thesis, Max-Planck-Institut für Quantenoptik, 2004.
[7] A. Pukhov, Phys. Rev. Lett. **86**, 3562 (2001).
[8] Y. Sentoku *et al.*, Phys. Plasmas **10**, 2009 (2003).
[9] P. Gibbon, Phys. Rev. E **72**, 026411 (2005).
[10] S. C. Wilks *et al.*, Phys. Plasmas **8**, 542 (2001).
[11] Y. Murakami, Phys. Plasmas **8**, 4138 (2001).
[12] M. Tabak *et al.*, Phys. Plasmas **1** (1994).
[13] I. Spencer *et al.*, CLF Annual Report (2001–2002), p. 19.
[14] T. Cowan *et al.*, Phys. Rev. Lett. **92**, 204801 (2004).
[15] P. Mora, Phys. Rev. Lett. **90**, 185002 (2003).
[16] V. T. Tikhonchuk *et al.*, Plasma Phys. Controlled Fusion **47**, B869 (2005).
[17] T. Z. Esirkepov *et al.*, Phys. Rev. Lett. **89**, 175003 (2002).
[18] M. Hegelich *et al.*, Bull. Am. Phys. Soc. **50**, 69 (2005).
[19] S. C. Wilks and W. L. Kruer, IEEE J. Quantum Electron. **33**, 1954 (1997).
[20] A. V. Gurevich *et al.*, Sov. Phys. JETP **22**, 499 (1966).
[21] L. Wickens and J. E. Allen, Phys. Rev. Lett. **41**, 243 (1978).
[22] M. Passoni *et al.*, Phys. Rev. E **69**, 026411 (2004).
[23] B. Bezzerides *et al.*, Phys. Fluids **21**, 2179 (1978).
[24] M. Borghesi *et al.*, Phys. Rev. Lett. **92**, 055003 (2004).